J|A|C|S ARTICLES

Published on Web 01/09/2009

Influence of the Lipidation Motif on the Partitioning and Association of N-Ras in Model Membrane Subdomains

Katrin Weise,[†] Gemma Triola,[‡] Luc Brunsveld,[‡] Herbert Waldmann,[‡] and Roland Winter[†,*]

Physical Chemistry I - Biophysical Chemistry and Chemical Biology, Faculty of Chemistry, Dortmund University of Technology, Otto-Hahn-Straβe 6, D-44227 Dortmund, Germany and Department of Chemical Biology, Max Planck Institute of Molecular Physiology, Otto-Hahn-Straβe 11, D-44227 Dortmund, Germany

Received November 5, 2008; E-mail: roland.winter@tu-dortmund.de

Abstract: In a combined chemical biological and biophysical approach using time-lapse tapping-mode atomic force microscopy, we studied the partitioning of differently lipidated N-Ras proteins with various membrane-localization motifs into lipid domains of canonical model raft mixtures. The results provide direct evidence that partitioning of N-Ras occurs preferentially into liquid-disordered lipid domains, independent of the lipid anchor system. N-Ras proteins bearing at least one farnesyl group have a comparable membrane partitioning behavior and show diffusion of the protein into the liquid-disordered/liquid-ordered phase boundary region, thus leading to a decrease of the unfavorable line tension between domains. In addition, except for the monofarnesylated N-Ras, strong intermolecular interactions foster self-association and formation of nanoclusters at the domain boundaries and may serve as an important vehicle for association processes and nanoclustering, which has also been observed in *in vivo* studies. No significant changes of the localization between GDP- and GTP-loaded N-Ras could be detected. Conversely, the nonbiological dual-hexadecylated N-Ras exhibits a time-independent incorporation into the bulk liquid-disordered phase to maintain high conformational entropy of its lipid chains.

1. Introduction

The lateral organization and intermolecular interactions of lipids and proteins in biological membranes are issues under heavy scrutiny in the fields of membrane biochemistry, biophysics, and cell biology.[1] The existence of membrane subdomains with different lipid composition and the relationship between lipid-domain formation and the conformation and functional properties of membrane-associated proteins is one of the central questions in this field.[1,2] The Ras proteins are lipidated membrane bound GTPases which in their active GTP-bound form mediate numerous growth factor related signaling events.[3−6] Misregulated Ras signaling is involved in the establishment of ca. 30% of human cancers.[7,8]

The three Ras isoforms H-, N-, and K-Ras are posttranslationally modified *via* lipidation on their C-termini, a modification which is essential for correct functioning and localization at the inner leaflet of the plasma membrane. The membrane anchors of H-, N-, and K-Ras comprise a common C-terminal *S*-farnesyl (Far) cysteine carboxy methylester, operating in concert with one or two adjacent *S*-palmitoyl (Pal) cysteine residues in N- and H-Ras, respectively, and with a polybasic stretch of six lysines in K-Ras.[8,9] Whereas farnesylation is a stable modification, palmitoylation is reversible. The lipidation is believed to play an important role in Ras regulatory functions, e.g., by mediating protein−protein and protein−lipid interactions. The association with different membrane microenvironments, including ordered raft domains, has been proposed to further regulate Ras signaling.[10−18]

[†] Physical Chemistry I - Biophysical Chemistry, Faculty of Chemistry, Dortmund University of Technology.

[‡] Department of Chemical Biology, Max Planck Institute of Molecular Physiology and Chemical Biology, Faculty of Chemistry, Dortmund University of Technology.

(1) Jacobson, K.; Mouritsen, O. G.; Anderson, R. G. *Nat. Cell Biol.* **2007**, *9*, 7–14.
(2) Munro, S. *Cell* **2003**, *115*, 377–388.
(3) Wittinghofer, A.; Pai, E. F. *Trends Biochem. Sci.* **1991**, *16*, 382–387.
(4) Kuhlmann, J.; Herrmann, C. Biophysical Characterization of the Ras Protein. In Topics in Current Chemistry. *Bioorganic Chemistry of Biological Signal Transduction*; Waldmann, H., Ed.; Springer: New York, 2001; Vol. 211; pp 61−116.
(5) Chiu, V. K.; Bivona, T.; Hach, A.; Sajous, J. B.; Silletti, J.; Wiener, H.; Johnson, R. L.; Cox, A. D.; Philips, M. R. *Nat. Cell Biol.* **2002**, *4*, 343–350.
(6) Bivona, T. G.; Philips, M. R. *Curr. Opin. Cell. Biol.* **2003**, *15*, 136–142.
(7) Bos, J. L. *Cancer Res.* **1989**, *49*, 4682–4689.
(8) Wittinghofer, A.; Waldmann, H. *Angew. Chem., Int. Ed.* **2000**, *39*, 4192–4214.
(9) Hancock, J. F.; Parton, R. G. *Biochem. J.* **2005**, *389*, 1−11.
(10) Zacharias, D. A.; Violin, J. D.; Newton, A. C.; Tsien, R. Y. *Science* **2002**, *296*, 913–916.
(11) Hancock, J. F. *Nat. Rev. Mol. Cell. Biol.* **2006**, *7*, 456–462.
(12) Abankwa, D.; Gorfe, A. A.; Hancock, J. F. *Semin. Cell. Dev. Biol* **2007**, *18*, 599–607.
(13) Pechlivanis, M.; Ringel, R.; Popkirova, B.; Kuhlmann, J. *Biochemistry* **2007**, *46*, 5341–5348.
(14) Wang, T.-Y.; Leventis, R.; Silvius, J. *Biophys. J.* **2000**, *79*, 919–933.
(15) Simons, K.; Toomre, D. *Nat. Rev. Mol. Cell. Biol.* **2000**, *1*, 31–39.
(16) Lobo, S.; Greentree, W. K.; Linder, M. E.; Deschenes, R. J. *J. Biol. Chem.* **2002**, *277*, 41268–41273.
(17) Zhao, L.; Lobo, S.; Dong, X. W.; Ault, A. D.; Deschenes, R. J. *J. Biol. Chem.* **2002**, *277*, 49352–49359.

It has been suggested that raft domains play a role in a wide range of important biological processes, including signal transduction pathways.[15,19] Such raft domains could also act as "signaling platforms" that couple events on the outside of the cell with signaling pathways inside the cell. In addition, recent theoretical and experimental work suggests that the interfacial line tension between domains may play a major role affecting membrane organization,[20,21] but there has been little evidence how this could affect lipoprotein partitioning and nanoclustering in membranes.

So far, essentially imaging approaches on intact plasma membranes have been used, and the structural properties of the lipid anchor systems have been proposed to control the partitioning properties in membrane subcompartments.[5,6,9−11,22] In an effort toward a molecular level understanding of the interaction of the Ras proteins with lipid domains, our focus has been to carry out biophysical studies aiming at analyzing the distribution of Ras lipoproteins with modified anchor systems in multiphasic artificial membrane structures. By using semisynthetic fully functional lipidated proteins,[23−29] e.g., a fluorescence labeled N-Ras bearing a farnesyl group and a hexadecyl moiety as a nonhydrolyzable mimic of the palmitoyl anchor (N-Ras HD/Far), the distribution of Ras between liquid-disordered and liquid-ordered (i.e., raft-like) subdomains and the orientation at the lipid interface were studied.[30−33] This led us to the formulation of a rule for preferred insertion of N-Ras HD/Far into membrane subdomains. Recent NMR-spectroscopic determination of the structure of the Ras protein bound to a one-component phospholipid bilayer revealed a detailed picture describing how the entire protein is embedded into a lipid bilayer.[34,35]

In this study we report on the influence of various N-Ras anchor systems, representing the major membrane-localization motifs as well as modifications thereof (HD/HD, HD/Far, Far/Far, and Far), on the partitioning of the protein into heterogeneous lipid bilayer membranes. As membrane heterogeneities may be as small as several tens of nanometers in natural membranes, and to yield a pictorial view of the localization process at the single molecule level, high-resolution imaging using tapping mode AFM has been used in our studies. Furthermore, the use of AFM has an additional advantage since there is no need of fluorescent labeling for visualization, thus avoiding a possible influence of the fluorophore on the results. To reveal also the kinetic behavior of the membrane association process we carried out time-lapse AFM measurements. Moreover, the influence of GTP/GDP loading on the localization of the N-Ras proteins in the heterogeneous lipid matrix has been explored, the reason being that evidence has been provided that H-Ras exhibits a GTP-dependent lateral segregation on the plasma membrane.[36,37] It was also suggested from experiments with monopalmitoylated H-Ras that the activation state may also play a role in the spatial localization of N-Ras.[38]

2. Materials and Methods

2.1. Sample Preparation. 2.1.1. Lipids. 1,2-Dioleoyl-*sn*-glycero-3-phosphocholine (DOPC) and 1,2-dipalmitoyl-*sn*-glycero-3-phosphocholine (DPPC) were purchased from Avanti Polar Lipids (Alabaster, USA), and cholesterol (Chol) was from Sigma-Aldrich (Deisenhofen, Germany). Stock solutions of 10 mg mL^{-1} lipid (DOPC, DPPC, and cholesterol) in chloroform (Merck, Darmstadt, Germany) were prepared and mixed to obtain 1.94 mg of total lipid with the desired composition of DOPC/DPPC/cholesterol 1:2:1 (molar ratio). The majority of the chloroform was evaporated with a nitrogen stream; all solvent was subsequently removed by drying under vacuum overnight.

2.1.2. N-Ras Proteins-Synthesis of Monofarnesylated N-Ras (N-Ras Far) and Double Lipidated N-Ras (N-Ras Far/Far, N-Ras Far/HD and N-Ras HD/HD).[23−29] Monofarnesylated N-Ras and double lipidated N-Ras peptides were synthesized with an *N*-terminal maleimide group *via* a combination of solution and solid phase strategies using either Fmoc-4-hydrazinobenzoyl NovaGel or 2-chlorotrityl resin. The maleimido peptides were coupled to a bacterially expressed truncated N-Ras protein (amino residues 1−181) carrying a cysteine at the C-terminus. Coupling was achieved by conjugate addition of the only surface-accessible cysteine(181)-SH group of N-Ras to the maleimido function.[39] Details on the nucleotide exchange on Ras proteins can be found in the Supporting Information.[40,41]

2.2. Atomic Force Microscopy. 2.2.1. Sample Preparation. For the AFM experiments with DOPC/DPPC/Chol membranes, the dry lipid mixture was hydrated with 1 mL of 20 mM Tris (Merck, Darmstadt, Germany), 5 mM $MgCl_2$ (Merck, Darmstadt, Germany), pH 7.4. The Tris buffer was filtered through Millipore filters of 0.02 μm pore size. The hydrated lipid mixture was then vortexed,

(18) Rocks, O.; Peyker, A.; Kahms, M.; Verveer, P. J.; Koerner, C.; Lumbierres, M.; Kuhlmann, J.; Waldmann, H.; Wittinghofer, A.; Bastiaens, P. I. *Science* **2005**, *307*, 1746–1752.
(19) Rajendran, L.; Simons, K. *J. Cell. Sci.* **2005**, *118*, 1099–1102.
(20) Kuzmin, P. I.; Akimov, S. A.; Chizmadzhev, Y. A.; Zimmerberg, J.; Cohen, F. S. *Biophys. J.* **2005**, *88*, 1120–1133.
(21) Garcia-Sáez, A. J.; Chiantia, S.; Schwille, P. *J. Biol. Chem.* **2007**, *16*, 33537–33544.
(22) Tian, T.; Harding, A.; Inder, K.; Plowman, S.; Parton, R. G.; Hancock, J. F. *Nat. Cell Biol.* **2007**, *9*, 905–914.
(23) Schelhaas, M.; Glomsda, S.; Hänsler, M.; Jakubke, H.-D.; Waldmann, H. *Angew. Chem., Int. Ed.* **1996**, *35*, 106–109.
(24) Nägele, E.; Schelhaas, M.; Kuder, N.; Waldmann, H. *J. Am. Chem. Soc.* **1998**, *120*, 6889–6902.
(25) Waldmann, H.; Nägele, E. *Angew. Chem., Int. Ed.* **1995**, *34*, 2259–2262.
(26) Kuhn, K.; Owen, D. J.; Bader, B.; Wittinghofer, A.; Kuhlmann, J.; Waldmann, H. *J. Am. Chem. Soc.* **2001**, *123*, 1023–1035.
(27) Kragol, G.; Lumbierres, M.; Palomo, J. M.; Waldmann, H. *Angew. Chem., Int. Ed.* **2004**, *43*, 5839–5842.
(28) Reents, R.; Wagner, M.; Kuhlmann, J.; Waldmann, H. *Angew. Chem., Int. Ed.* **2004**, *43*, 2711–2714.
(29) Brunsveld, L.; Kuhlmann, J.; Alexandrov, K.; Wittinghofer, A.; Goody, R. S.; Waldmann, H. *Angew. Chem., Int. Ed.* **2006**, *45*, 6622–6646.
(30) Fahsel, S.; Pospiech, E.-M.; Zein, M.; Hazlett, T. L.; Gratton, E.; Winter, R. *Biophys. J.* **2002**, *83*, 334–344.
(31) Janosch, S.; Nicolini, C.; Ludolph, B.; Peters, C.; Völkert, M.; Hazlet, T. L.; Gratton, E.; Waldmann, H.; Winter, R. *J. Am. Chem. Soc.* **2004**, *126*, 7496–7503.
(32) Nicolini, C.; Baranski, J.; Schlummer, S.; Palomo, J.; Lumbierres-Burgues, M.; Kahms, M.; Kuhlmann, J.; Sanchez, S.; Gratton, E.; Waldmann, H.; Winter, R. *J. Am. Chem. Soc.* **2006**, *128*, 192–201.
(33) Meister, A.; Nicolini, C.; Waldmann, H.; Kuhlmann, J.; Kerth, A.; Winter, R.; Blume, A. *Biophys. J.* **2006**, *91*, 1388–1401.
(34) Reuther, G.; Tan, K. T.; Vogel, A.; Nowak, C.; Arnold, K.; Kuhlmann, J.; Waldmann, H.; Huster, D. *J. Am. Chem. Soc.* **2006**, *128*, 13840–13846.
(35) Vogel, A.; Tan, K. T.; Waldmann, H.; Feller, S. E.; Brown, M. F.; Huster, D. *Biophys. J.* **2007**, *93*, 2697–2712.
(36) Prior, I. A.; Muncke, C.; Parton, R. G.; Hancock, J. F. *J. Cell. Biol.* **2003**, *160*, 165–170.
(37) Prior, I. A.; Harding, A.; Yan, J.; Sluimer, J.; Parton, R. G.; Hancock, J. F. *Nat. Cell Biol.* **2001**, *3*, 368–375.
(38) Roy, S.; Plowman, S.; Rotblat, B.; Prior, I. A.; Muncke, C.; Grainger, S.; Parton, R. G.; Henis, Y. I.; Kloog, Y.; Hancock, J. F. *Mol. Cell. Biol.* **2005**, *25*, 6722–6733.
(39) Bader, B.; Kuhn, K.; Owen, D. J.; Waldmann, H.; Wittinghofer, A.; Kuhlmann, J. *Nature* **2000**, *403*, 223–226.
(40) Lenzen, C.; Cool, R. H.; Prinz, H.; Kuhlmann, J.; Wittinghofer, A. *Biochemistry* **1998**, *37*, 7420–7430.
(41) Lenzen, C.; Cool, R. H.; Wittinghofer, A. *Methods Enzymol.* **1995**, *225*, 95–109.

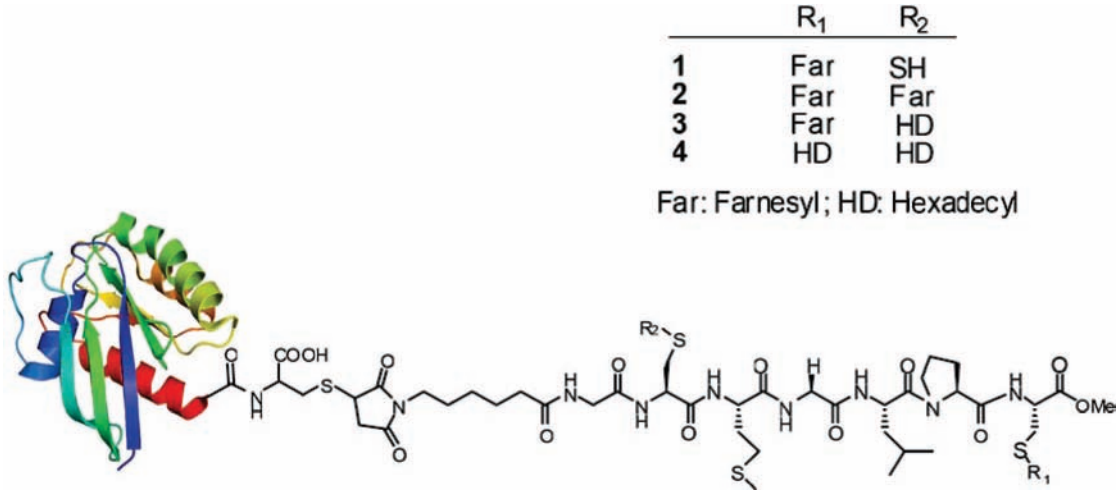

Figure 1. Schematic of the semisynthetic N-Ras protein with the different anchor systems. The abbreviations for the residues R_1 and R_2 refer to hexadecyl (HD, as a nonhydrolyzable palmitoyl group analog) and farnesyl (Far).

kept in a water bath at 65 °C for 15 min, and sonicated for 10 min. After five freeze−thaw−vortex cycles and brief sonication, large multilamellar vesicles were formed and transformed to large unilamellar vesicles of homogeneous size by use of an extruder (Avanti Polar Lipids, Alabaster, USA) with polycarbonate membranes of 100 nm pore size at 65 °C. Supported lipid bilayers for AFM measurements were produced by depositing 30 μL of the lipid vesicle solution together with 40 μL of Tris buffer on freshly cleaved mica and incubation in a wet chamber at 70 °C for 2 h. After vesicle fusion, the sample was rinsed carefully with Tris buffer to remove excess unspread vesicles and placed on the AFM stage. For the protein−lipid interaction studies, 200 μL of N-Ras protein in Tris buffer ($c = 100\ \mu g\ mL^{-1}$) were slowly injected into the AFM fluid cell and allowed to incubate for 1 h at room temperature, a time frame that turned out to be appropriate for membrane interaction AFM studies in general. Afterward, the fluid cell was rinsed carefully with Tris buffer before imaging to remove unbound protein. With this technique, imaging of the same sample region before and after protein injection is possible.

2.2.2. AFM Setup. Measurements were performed on a MultiMode scanning probe microscope with a NanoScope IIIa controller (Digital Instruments, Santa Barbara, CA, USA) and usage of a J-Scanner (scan size 125 μm), the latter allowing the parallel imaging of three independent 100 μm^2 sample regions for each set of measurements to ensure reliability of the data. Images were obtained by applying the Tapping Mode in liquid with oxide-sharpened silicon nitride probes (DNP-S, Veeco Instruments, Mannheim, Germany) mounted in a fluid cell (MTFML, Veeco Instruments, Mannheim, Germany). Tips with nominal force constants of 0.32 N/m were used at driving frequencies around 9 kHz and drive amplitudes between 200 and 400 mV. The same AFM tip was used for each set of experiments throughout. This is generally due to the experimental setup which does not allow for cantilever changes during measurements without damaging the membrane sample and losing the exact imaging region as scanned before. Height and phase images of sample regions were acquired with resolutions of 512 × 512 pixels. Owing to the general properties of such soft matter samples, slow scan frequencies between 0.5 and 1.5 Hz were required for high resolution images. All measurements were carried out at room temperature. The partitioning of the lipidated proteins was analyzed by use of image analysis and processing software (NanoScope version 5 and Origin).

3. Results

With the aim of studying the influence of the Ras lipid membrane anchors on membrane distribution, different N-Ras proteins were prepared using chemical biology strategies that gave access to the fully lipidated proteins and additional non-natural modifications. To this end, monofarnesylated N-Ras (N-Ras Far) and double lipidated N-Ras (N-Ras Far/Far, N-Ras Far/HD, and N-Ras HD/HD) were obtained by a combination of solution and solid phase synthesis of peptides followed by ligation to an expressed Ras protein (Figure 1).

At the beginning of each set of time-lapse AFM measurements, a sample consisting of a pure DOPC/DPPC/cholesterol lipid bilayer with a molar ratio of 1:2:1 was examined to ensure formation of a homogeneous sample with coexisting liquid-ordered (l_o) and liquid-disordered (l_d) domains and the absence of membrane defects. In all cases shown, the AFM images exhibit one homogeneous lipid bilayer with coexisting l_o and l_d domains (Figure 2 and Figure S1 in the Supporting Information). The thickness of the lipid bilayer is ∼5.0 nm for the l_o phase and ∼4.0 nm for the l_d phase; i.e., the coexisting phases can be clearly distinguished by a height difference of ∼1.0 nm (Figure 2, section analysis), in agreement with literature data.[42] In the AFM image, isolated islands of fluid l_d domains (dark brown) are clearly visible in a coherent pool of raft-like (l_o) protruding phase (light brown). Hence, the location of the protein particles can be clearly assigned to either l_d or l_o domain areas.

Using the technique of direct injection of a solution containing N-Ras protein into the AFM fluid cell, the same region of the lipid bilayer can be observed before and after incorporation of the protein. Owing to the absence of convection, the diffusion process to the lipid interface is rather slow so that kinetic AFM measurements can be conducted. AFM measurements were carried out at several time points after addition of protein with the first images taken after ∼ 1.0 h as a consequence of the protein incubation procedure. The following figures shown comprise a selection of images at particular time points which represent the main features of the membrane partitioning processes detected, i.e., the different scenarios observed for the different Ras anchor motifs. In Figure 3, AFM images at different times after protein injection are shown for the N-Ras HD/Far, N-Ras Far/Far and N-Ras HD/HD. It is clearly visible that the incubation of the lipid bilayer with farnesylated N-Ras protein (Far/Far and HD/Far) solution changes the lateral organization of the membrane within the first three hours after adding the protein. The addition of the protein solution leads

(42) Rinia, H. A.; Snel, M. M. E.; Van der Eerden, J. P. J. M.; de Kruijff, B. *FEBS Lett.* **2002**, *501*, 92–96.

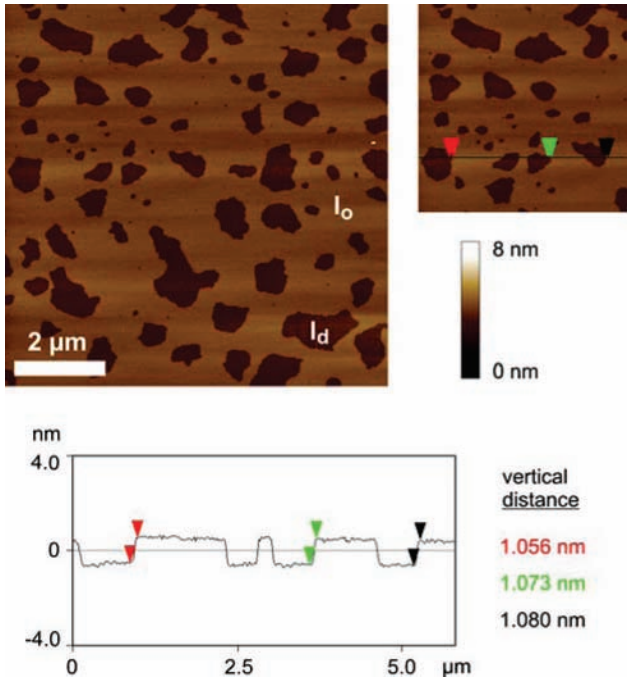

Figure 2. AFM image of a DOPC/DPPC/Chol 1:2:1 lipid membrane on mica before injection of protein solution. In the upper part, the whole scan area is shown with a vertical color scale from dark brown to white corresponding to an overall height of 8 nm and indicating a homogeneous lipid bilayer with coexisting domains in l_o and l_d phase. The concomitant section profile of the AFM image is given at the bottom. The horizontal black line in the figure on the right-hand side is the localization of the section analysis shown at the bottom, indicating the vertical distances between pairs of arrows (black, green, and red).

to an increase in the amount of l_d phase, whereas the formerly dominant l_o domain areas decrease concomitantly, meaning that the situation is inverted ~3 h after protein incorporation: now isolated islands of l_o phase are surrounded by a coherent l_d phase containing the protein (relative areas are given in the Supporting Information, Table S1). In the AFM images at time $t \approx 2.0$ h and $t \approx 2.5$ h, three types of domains can be distinguished: l_d areas with incorporated protein (dark-brown background), l_d domains without protein (small brown areas), and l_o domains without protein (light brown areas). The height differences between the domains are 2.2 ± 0.2 nm for $l_d - l_d$(+protein) and 3.4 ± 0.2 nm for $l_o - l_d$(+protein) in the case of N-Ras Far/Far and 2.4 ± 0.2 nm for $l_d - l_d$(+protein) and 3.3 ± 0.2 nm for $l_o - l_d$(+protein) in the case of N-Ras HD/Far (Table 1). Thus, the difference between the l_o phase and the l_d phase without incorporated protein is still ~1.0 nm. Remarkably, the thickness of the lipid membrane decreases significantly upon incorporation of the farnesylated N-Ras proteins into the fluid lipid phase, which might be largely due to a decrease of conformational order of the lipid bilayer with concomitant lateral expansion upon incorporation of the lipidated protein. This would be in accord with the expected influence of the bulky farnesyl chain and the low chain order parameter profiles of the hexadecyl chain as observed in ^{2}H NMR experiments for N-Ras and Ras peptide mimetics in DMPC bilayers.[34,35]

The data also show that the incorporated lipidated proteins N-Ras Far/Far and N-Ras HD/Far are nearly exclusively located in the bulk l_d phase and exhibit a mean height of 2.7 ± 0.6 and 2.6 ± 0.5 nm (Table 1), respectively, which corresponds roughly to the linear dimension of a N-Ras molecule. However, after 20 h with ~10 h in the nonoperative mode, i.e., without disturbance due to the AFM scanning process, diffusion of the N-Ras proteins to the phase boundaries was observed (Figure 3, $t \approx 25.0$ and 26.0 h). The incorporation of the farnesylated N-Ras proteins into the l_d/l_o domain boundary region and subsequent clustering result in a decrease of the line energy (tension) between the domains which is energetically favorable and reflected in a decrease in the initial height difference between the l_o phase and l_d phase with incorporated protein (Table 1), meaning that the l_o islands are lowered (they become darker in the color code used). However, the shape and relative amount of the lipid domains stay nearly constant. Whereas the size of the protein particles located in the l_d bulk phase remains nearly constant, an increase in the size of N-Ras Far/Far and N-Ras HD/Far to 6.2 ± 1.6 and 4.8 ± 1.4 nm, respectively, can be detected when they cluster in the interfacial region of the domains. The described effects are enhanced when the system is left for an additional 20 h (~10 h in the operative and ~10 h in the nonoperative mode, i.e., no scanning; Figure 3, $t \approx 41.5$ h and $t \approx 45.0$ h). After ~42 h, a coherent l_d phase with incorporated N-Ras Far/Far proteins (which can be clearly detected as light dots) is visible that encloses dark islands without protein that were previously l_o domains. Since these domains do not show characteristic properties of l_o domains any more, i.e., the characteristic height difference of 1.0 nm, and are now lower in height (0.6 nm, Table 1) than the surrounding l_d domains with incorporated protein, we refer to them at this stage as fluid domains without protein. Hence, almost no l_o domains can be found at the end of the protein partitioning process, meaning that the l_o/l_d phase coexistence detected at the beginning of the experiment is abolished by the accumulation of the protein in the domain interface. These results agree very well with a previous comparative fluorescence and atomic force microscopy study using fluorescence labeled N-Ras HD/Far and analyzing the distribution of Ras between l_d and l_o subdomains.[32] The experiments led to the formulation of a rule for preferred insertion of N-Ras HD/Far into membrane subdomains with a large proportion of the N-Ras protein residing in the l_d/l_o phase boundary region.

In contrast to the farnesylated N-Ras proteins, no change in the phase behavior and lateral organization of the lipid bilayer can be observed for the dually hexadecylated N-Ras protein. After incubation of the membrane with N-Ras HD/HD, coexisting l_d and l_o phases of similar shape and size can still be distinguished for the whole time range covered. The height difference between both phases stays constant at ~1.0 nm. The N-Ras HD/HD can be targeted protruding in bulk l_d domains with a height of 2.1 ± 0.8 nm (Table 1). Surprisingly, for the N-Ras HD/HD, no lateral diffusion of the protein into the interfacial region of the coexisting domains and no clustering could be detected. Even at $t \approx 41.5$ h, the protein size and height difference of phases stay nearly constant (2.2 and 1.0 nm, respectively).

A similar partitioning mechanism of the protein particles as for N-Ras HD/Far and N-Ras Far/Far could be detected for the monofarnesylated N-Ras. Again, the incubation of the lipid bilayer with the N-Ras Far solution changes the lateral membrane organization within the first 2.5 h in showing an increase in l_d phase, whereas the formerly dominant l_o domains vanish. Also, the incorporation of the monofarnesylated N-Ras protein into the fluid phase (l_d) results in a thinning of the lipid membrane thickness. The data reveal a nearly exclusively partitioning of N-Ras Far in the bulk l_d phase, with a mean height of 2.8 ± 0.8 nm, and with time, diffusion of the N-Ras

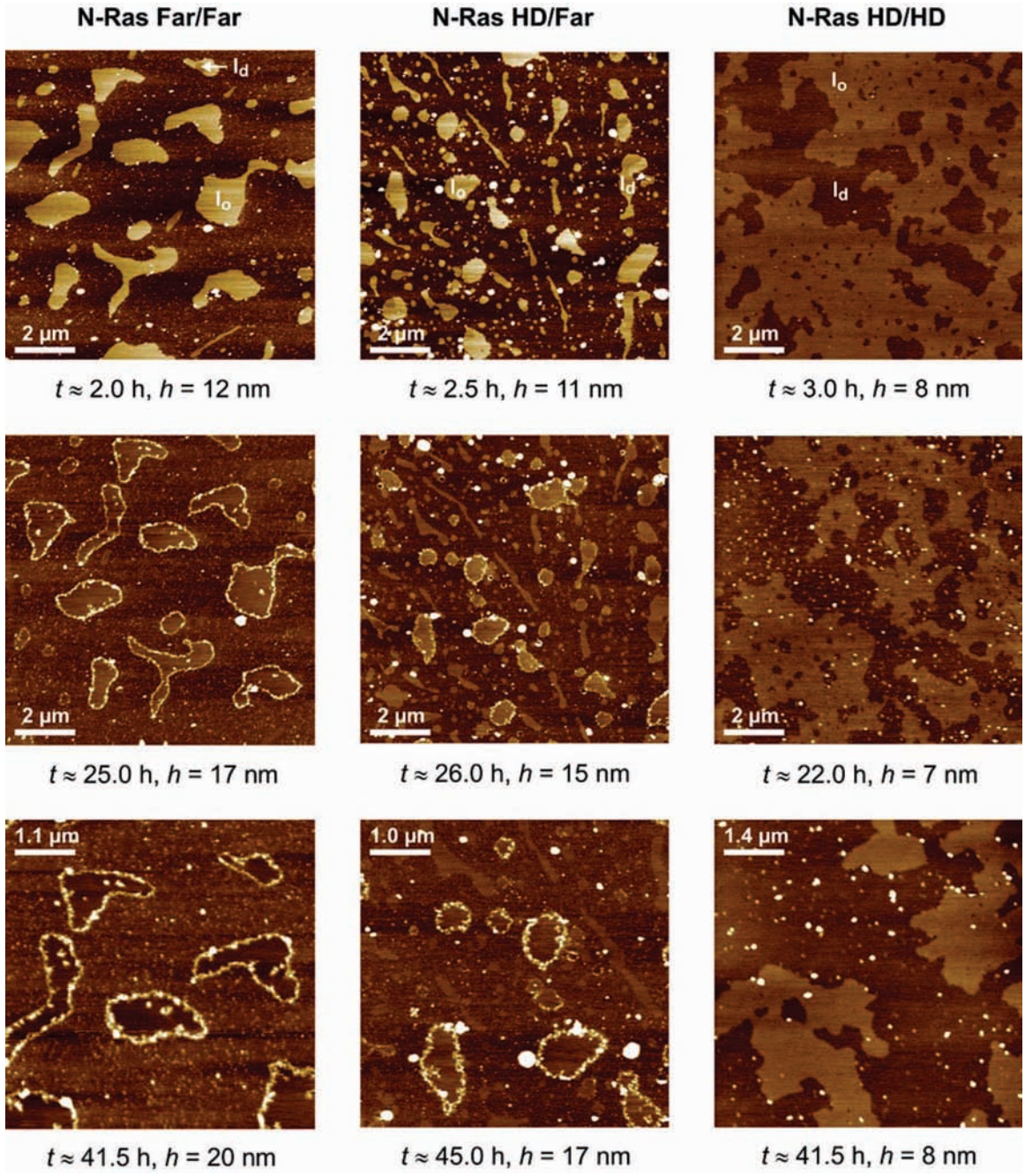

Figure 3. AFM images of the time-dependent partitioning of N-Ras Far/Far, N-Ras HD/Far, and N-Ras HD/HD into lipid bilayers consisting of DOPC/DPPC/Chol 1:2:1. The AFM images are shown at a particular time after injection of 200 μL of N-Ras Far/Far, N-Ras HD/Far, and N-Ras HD/HD in 20 mM Tris, 5 mM $MgCl_2$, pH 7.4 ($c = 100$ μg mL^{-1}) into the AFM fluid cell. h gives the overall height of the vertical color scale.

Far proteins to the domain boundaries is detected (Figure 4, Table 1). The size of the N-Ras Far in the bulk l_d phase and in the phase boundary region remains constant over the whole time range, indicating that, in contrast to the N-Ras Far/Far and N-Ras HD/Far scenario, no pronounced clustering is observed for the N-Ras Far.

Comparing the membrane partitioning of the GDP-bound N-Ras HD/Far (as described above) and the GTP-activated analog (GppNHp-bound state as a nonhydrolyzable GTP analog), a similar behavior is observed (Figure 4). Both proteins exhibit similar changes in lateral membrane organization within the first three hours. Neither the GDP-bound nor the GTP-activated N-Ras HD/Far can be detected in the bulk raft-like l_o phase, instead, both proteins are located nearly exclusively in the bulk l_d phase. Notably, the GTP-activated N-Ras HD/Far has a mean height of 5.9 ± 1.7 nm, which is roughly twice the height of GDP-bound N-Ras HD/Far (2.6 ± 0.5 nm, Table 1). This size difference could be explained by different conformations of the GDP- and GTP-complexed N-Ras proteins, which might lead to a different orientation of the protein at the lipid interface and to a change in intermolecular interactions and protein self-association. Both the GDP- and the GTP-bound N-Ras HD/Far protein diffuse to and cluster in the domain boundaries with time, resulting in a comparable decrease in the initial height difference between the l_o phase and the l_d phase with protein and between the l_d phase without protein and the l_d phase with protein, respectively (Figure 4, Table 1). GTP-

Table 1. Analysis of the AFM Images at Different Time Points after Protein Injection, Giving the Mean Size of the N-Ras Protein and the Height Difference between Lipid Phases[a]

	$size_{pb} \pm SD$	n_{pb}	$size_{pi} \pm SD$	n_{pi}	Δh
			N-Ras HD/HD		
$t \approx 3.0$ h	−	−	−	−	1.0 ± 0.1 nm
$t \approx 22.0$ h	2.1 ± 0.8 nm	229	−	−	1.0 ± 0.1 nm
$t \approx 41.5$ h	2.2 ± 1.0 nm	88	−	−	1.0 ± 0.1 nm
			N-Ras HD/Far		
$t \approx 2.5$ h	2.6 ± 0.5 nm	145	−	−	3.3 ± 0.2 nm
$t \approx 26.0$ h	3.2 ± 1.1 nm	67	4.8 ± 1.4 nm	234	1.5 ± 0.2 nm
$t \approx 45.0$ h	3.8 ± 1.0 nm	113	6.4 ± 1.6 nm	231	1.1 ± 0.2 nm
			N-Ras Far/Far		
$t \approx 2.0$ h	2.7 ± 0.6 nm	173	−	−	3.4 ± 0.2 nm
$t \approx 25.0$ h	2.9 ± 0.8 nm	216	6.2 ± 1.6 nm	366	1.2 ± 0.2 nm
$t \approx 41.5$ h	3.0 ± 0.9 nm	206	7.5 ± 2.0 nm	299	-0.6 ± 0.4 nm
			N-Ras Far		
$t \approx 2.5$ h	2.8 ± 0.8 nm	82	−	−	2.8 ± 0.2 nm
$t \approx 22.0$ h	2.2 ± 0.8 nm	140	2.0 ± 0.4 nm	272	0.5 ± 0.1 nm
$t \approx 47.0$ h	2.2 ± 0.6 nm	90	2.3 ± 0.6 nm	284	0.5 ± 0.1 nm
			N-Ras HD/Far GTP		
$t \approx 3.5$ h	5.9 ± 1.7 nm	215	−	−	2.2 ± 0.2 nm
$t \approx 24.0$ h	5.9 ± 2.2 nm	175	5.2 ± 1.3 nm	262	1.2 ± 0.1 nm
$t \approx 44.5$ h	5.2 ± 2.0 nm	138	4.6 ± 1.2 nm	215	1.2 ± 0.1 nm

[a] For the height difference between the lipid phases, Δh, the mean value with the standard deviation is given ($n = 42-72$). The phase difference describes the difference in height between the l_o and l_d phase in the case of N-Ras HD/HD, between the l_o phase and l_d phase with incorporated protein for N-Ras HD/Far, N-Ras Far/Far, as well as N-Ras Far, and between the l_d phase without protein and the l_d phase with incorporated protein for N-Ras HD/Far GTP. n_{pb} and n_{pi} give the number of protein particles in the bulk (b) phase and interface (i), respectively, used to calculate the corresponding mean values ± SD (standard deviation), which is not in each case identical with the total number of protein particles seen in the AFM image.

bound N-Ras HD/Far differs from GDP-bound N-Ras HD/Far in showing some extent of clustering also in the bulk fluid phase.

4. Discussion

By using time-lapse tapping-mode AFM, we were able to detect the partitioning of N-Ras lipoproteins with various membrane-localization motifs into lipid domains of canonical model raft mixtures. The results provide direct evidence that partitioning of GDP-loaded N-Ras occurs preferentially into liquid-disordered lipid domains, independent of the lipid anchor system (Far/Far, HD/Far, HD/HD, Far). Upon incorporation of the single- and double-farnesylated N-Ras proteins, the thickness of the fluid bilayer decreases due to membrane disordering.

Furthermore, we were able to demonstrate that GDP-loaded N-Ras proteins bearing at least one farnesyl anchor (N-Ras Far/Far, N-Ras HD/Far, N-Ras Far) have comparable membrane partitioning behavior and show diffusion of the protein into the l_o/l_d phase boundary region with time. We may propose that the farnesyl anchor is largely responsible for the clustering of N-Ras proteins in the interfacial regions of membrane domains (Figure 5), thus leading to a decrease of the line energy (tension) between domains. Upon insertion at the interfacial domain boundaries, the line tension between domains decreases, which in fact depends quadratically on the phase height mismatch.[20] Notably, no pronounced clustering is observed for the mono-farnesylated N-Ras Far, which is less stably inserted into the lipid membrane. Hence, line tension is likely to be one of the key parameters controlling not only the size and dynamic properties of rafts[21] but also signaling platforms. Owing to the prevalence of interfaces in natural membranes, this general physicochemical line tension effect that we have observed is likely to be extendable to the plasma membrane situation as well. Such an interfacial adsorption effect can generally be expected in many-phase lipid systems for inserting proteins that have no particular preference for any particular phase[43−45]—for example due to hydrophobic mismatch and/or due to entropic reasons—so that the proteins are expelled to the boundary. It is clear that the localization and accumulation of proteins in the domain interfaces of a lipid bilayer increase the effective concentration and may provide particularly strong and direct protein−protein interactions and hence may serve as an important vehicle for association processes of signaling proteins in membranes.

Conversely, the dual-hexadecylated N-Ras exhibits a time-independent incorporation into the bulk liquid-disordered phase. It might have been envisaged that the N-Ras HD/HD protein with its long saturated and unbranched lipid chains is prone to partition into ordered raft-like domains. This is clearly not the case. The most likely explanation is that by remaining in the fluid-like phase and being integrated in the collective flexibility and dynamics of the lipid bilayer, the high conformational entropy of the two lipid chains separated by a dynamic peptide linker is retained. As revealed by recent NMR experiments, such an effect is probably fostered by the high-amplitude dynamics of the C-terminal peptide linker region.[34,35] Thus, only the more rigid but bulkier farnesyl moiety of the N-Ras protein seems to be essential for interfacial self-association and formation of nanoclusters. Such an effective concentration of signaling proteins into discrete nanodomains in the membrane may in fact be expected to increase the efficiency and specificity of signaling events. Interestingly, besides a high population of monomers, nanoclusters of similar sizes (radius of ~6−12 nm) have been found in the plasma membrane as well.[11,22,48]

It is assumed that N-Ras Far and N-Ras HD/Far resemble the depalmitoylated and palmitoylated forms of the natural N-Ras, respectively, in terms of the chemical nature of the lipid anchors. Palmitoyl and hexadecyl differ only in the thioester and thioether bond connecting the fatty acid chain with the Ras peptide; the saturation, conformation, and length of the fatty acid chains are identical. Thus, similar interactions of these membrane anchors with the canonical raft membranes can be envisaged. Concerning our finding that GDP-loaded N-Ras HD/Far and N-Ras Far display a similar membrane partitioning behavior, we propose that the main function of the natural palmitoyl anchor of N-Ras resides predominantly in the residence time in a particular cellular membrane compartment in the course of the acylation/deacylation cycle. This acylation/deacylation cycle was discovered recently and revealed that the dynamic property of the palmitate moiety, i.e., the reversibility of palmitoylation, is critical for the correct localization of N-Ras in a particular cellular membrane, such as the Golgi or plasma

(43) Nielsen, L. K.; Vishnyakov, A.; Jørgensen, K.; Bjørnholm, T.; Mouritsen, O. G. *J. Phys.: Condens. Matter* **2000**, *12*, A309–A314.
(44) Zuckermann, M. J.; Ipsen, J. H.; Miao, L.; Mouritsen, O. G.; Nielsen, M.; Polson, J.; Thewalt, J.; Vattulainen, I.; Zhu, H. *Methods Enzymol.* **2004**, *383*, 198–229.
(45) Khandelia, H.; Ipsen, J. H.; Mouritsen, O. G. *Biochim. Biophys. Acta, Biomembr.* **2008**, *1778*, 1528–1536.
(46) Völkert, M.; Wagner, M.; Peters, C.; Waldmann, H. *Biol. Chem.* **2001**, *382*, 1133–1145.
(47) Mitin, N.; Rossman, K. L.; Der, C. J. *Curr. Biol.* **2005**, *15*, R563–R574.
(48) Plowman, S. J.; Hancock, J. F. *Biochim. Biophys. Acta, Mol. Cell. Res* **2005**, *1746*, 274–283.

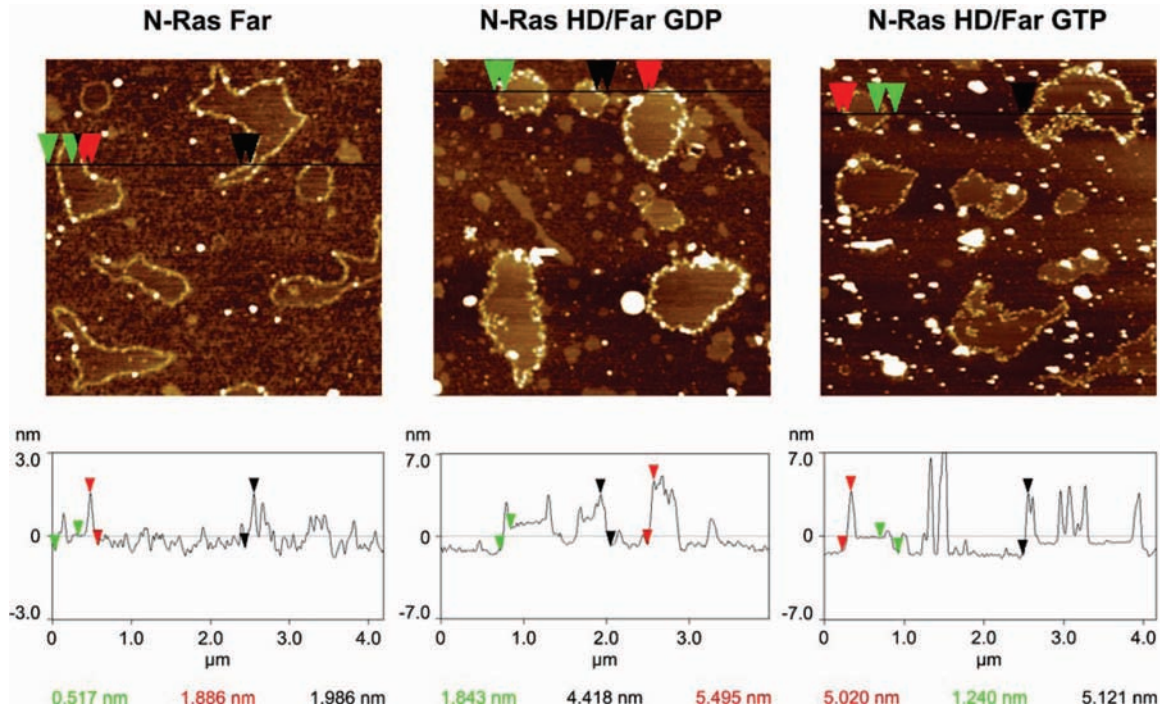

Figure 4. AFM images of GDP-bound N-Ras Far, GDP-bound N-Ras HD/Far, and the GTP-activated analog (GppNHp-bound state) N-Ras HD/Far at $t \approx$ 22.0, 26.0, and 24.0 h after addition of protein, respectively. In the upper part, the section profile of the AFM image is shown with a vertical color scale from dark brown to white corresponding to an overall height of 6, 14, and 14 nm for the N-Ras Far, N-Ras HD/Far, and N-Ras HD/Far GTP, respectively. The horizontal black line is the localization of the section analysis shown at the bottom, indicating the vertical distances between pairs of arrows (black, green, and red).

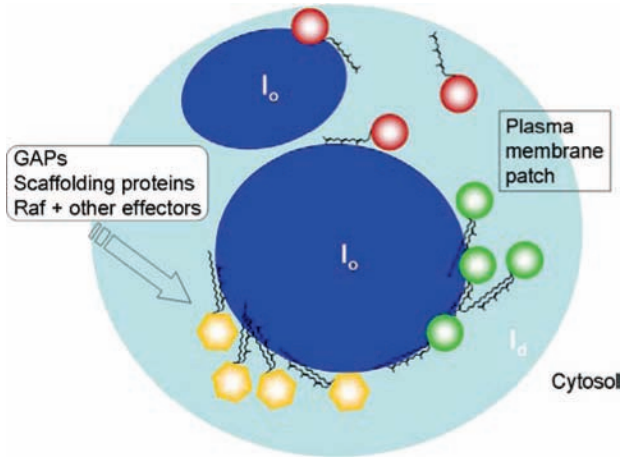

Figure 5. Model for N-Ras localization in heterogeneous membranes with liquid-disordered (l_d, light blue) and liquid-ordered (l_o, blue) domains. GDP-loaded farnesylated Ras (red) partitions into the fluid-like phase of the membrane and subsequently diffuses to the l_d/l_o phase boundaries of the subcompartments. When Ras is farnesylated and palmitoylated (green), strong intermolecular interactions foster self-association and formation of nanoclusters at the domain boundaries, which might serve as a reaction platform for GTP activation (yellow) and for recruitment of further membranous and cytosolic regulators as well as downstream effectors of the Ras signaling pathway, such as Gap and Raf.[29,46,47] In addition, scaffolding proteins might be involved in this process.

membrane.[18,49] Farnesylation alone is not sufficient to stably anchor Ras to the plasma membrane, so loss of palmitate will lead to dissociation of Ras from the plasma membrane. The stability of palmitate attachment thereby dictates the steady-state distribution and the speed of exchange of the plasma membrane and Golgi pools.[18,50] The cycle has been proposed to operate independently of the activation state of Ras. In fact, our data point to such behavior also in the heterogeneous model membrane system studied, as no significant changes of the localization between GDP- and GTP-loaded N-Ras HD/Far could be detected. GTP-bound N-Ras HD/Far differs from GDP-bound N-Ras HD/Far in showing different clustering propensities, only. These results are in contrast to previous experiments using a monopalmitoylated H-Ras as a N-Ras mimetic, which suggested that GTP/GDP-loading might influence the plasma membrane microdomain localization of N-Ras analogous to H-Ras.[38] However, recently it was demonstrated that H-Ras contains in addition to the lipid anchor two further domains that regulate the membrane association of H-Ras: the hypervariable linker domain and the N-terminal catalytic domain, with the latter being modulated by conformational changes caused by GTP-loading.[51] Whereas the N-terminal G-domain of H-Ras has been shown to influence the localization of H-Ras within the plane of the plasma membrane,[51] there is evidence that the N-Ras G-domain regulates gross compartmentalization (subcellular localization).[52] Therefore, the N-terminal domain does not seem to influence the plasma membrane microdomain localization of N-Ras, which is also supported by our recent data and previous experiments studying the membrane partitioning behavior of lipidated N-Ras peptides corresponding to the C-terminal segment of N-Ras (unpublished results and ref 31).

(49) Goodwin, J. S.; Drake, K. R.; Rogers, C.; Wright, L.; Lippincott-Schwartz, J.; Philips, M. R.; Kenworthy, A. K. *J. Cell. Biol.* **2005**, *170*, 261–272.
(50) Rocks, O.; Peyker, A.; Bastiaens, P. I. H. *Curr. Opin. Cell. Biol.* **2006**, *18*, 351–357.
(51) Rotblat, B.; Prior, I. A.; Muncke, C.; Parton, R. G.; Kloog, Y.; Henis, Y. I.; Hancock, J. F. *Mol. Cell. Biol.* **2004**, *24*, 6799–6810.
(52) Laude, A. J.; Prior, I. A. *J. Cell. Sci.* **2008**, *121*, 421–427.

To conclude, the aim of this study was to understand the mechanism of interaction of different lipidated proteins, i.e., the membrane-localization motif itself, with lipid domains of canonical model raft mixtures. This issue has been a matter of severe debate in past years, in particular in cell biological studies, where, owing to the complexity of the system, such interaction mechanisms are difficult to reveal. Certainly, the observed interaction processes occur on a faster time scale *in vivo* due to a different dynamics in the complex biological cell compared to an AFM fluid cell. However, the underlying biophysical mechanism for the partitioning process will not be influenced by the different dynamics. Moreover, previous studies have shown that the spontaneous intermembrane transfer of dually lipid anchored Ras peptides may also occur on the order of hours.[53] Even if the *in vivo* acylation/deacylation cycle is not present in this model system, a general understanding of the interaction mechanism of membrane anchored proteins with heterogeneous raft membranes is gained from our study. These data also provide the basis for further studies involving different types of cellular interaction partners with Ras, like Raf and other effectors, which will aid in interpreting cell biological work on Ras signaling.

Acknowledgment. We thank Christine Nowak for excellent technical assistance. Financial support from the Deutsche Forschungsgemeinschaft (SFB 642) and the Fonds der Chemischen Industrie is gratefully acknowledged. G.T. thanks Generalitat de Catalunya for a Postdoctoral Fellowship. L.B. was supported by a Sofja Kovalevskaja Award of the Alexander von Humboldt Foundation and the BMBF.

Supporting Information Available: N-Ras Synthesis: General aspects, general procedure for the synthesis of lipidated peptides using Fmoc-4-hydrazinobenzoyl NovaGel resin (**1**+**2**), general procedure for the synthesis of lipidated peptides using 2-chlorotrityl resin (**3**+**4**), and characterization of lipopeptides **1**, **2**, **3**, and **4**. AFM images for all N-Ras proteins at $t = 0$ h (Figure S1) and analysis of the AFM images before ($t = 0$ h) and after protein injection ($t = 2.0-3.5$ h) regarding the relative areas of l_o and l_d phases (Table S1). This material is available free of charge via the Internet at http://pubs.acs.org.

JA808691R

(53) Schroeder, H.; Leventis, R.; Rex, S.; Schelhaas, M.; Nägele, E.; Waldmann, H.; Silvius, J. R. *Biochemistry* **1997**, *36*, 13102–13109.